J|A|C|S
ARTICLES
Published on Web 01/24/2007

Probing Side-Chain Dynamics in the Proteasome by Relaxation Violated Coherence Transfer NMR Spectroscopy

Vitali Tugarinov, Remco Sprangers, and Lewis E. Kay*

Contribution from the Departments of Medical Genetics, Biochemistry and Chemistry, The University of Toronto, Toronto, Ontario, Canada M5S 1A8

Received November 1, 2006; E-mail: kay@pound.med.utoronto.ca

Abstract: A pair of experiments is presented for measuring intra-methyl $^1H-^1H$ dipolar cross-correlated spin relaxation rates in highly deuterated, methyl protonated proteins with significantly improved sensitivity relative to previously developed experiments that measure dynamics via ^1H spin relaxation. In applications to proteins with correlation times in the macromolecular limit, these cross-correlation rates are related directly to order parameters, characterizing the amplitude of motion of methyl-containing side-chains. The experimental approach is validated by comparing extracted order parameters with those obtained via ^2H and ^{13}C spin relaxation methods for both protein L (7.5 kDa) and malate synthase G (82 kDa), with excellent correlations obtained. The methodology is applied to study Ile, Leu, and Val side-chain dynamics in a 360 kDa "half-proteasome" complex. In particular, order parameters obtained from the WT complex and from a second complex where the proteasome gating residues are deleted establish that the relative levels of dynamics in each of the two molecules are very similar. It thus becomes clear that there is no communication between gating residues and other regions of the molecule involving pico- to nanosecond time-scale dynamics of these methyl-containing side-chains.

Introduction

Protein function is often intimately coupled to molecular dynamics.[1] For example, protein motions are integral to the thermodynamic stability of functional states,[2] to catalysis,[3] to ligand binding,[4] to molecular recognition processes,[5] and to allostery.[6] One system where dynamics are likely to be critical is the 20S proteasome (20S CP), a 700 kDa molecular machine that plays a critical role in the removal of damaged and misfolded proteins from the cell and that regulates crucial cellular processes such as cell division, gene expression, signal transduction, and apoptosis.[7,8] X-ray studies of the 20S CP establish an architecture in which four heptameric rings are stacked one on top of the other,[9−11] Figure 1a, to form an α_7-β_7-β_7-α_7 ring structure, with a pair of antechambers sandwiching the catalytic chamber where protein degradation occurs. Despite the detailed crystallographic studies of the 20S CP from a number of different organisms, in the free form[9−11] and in complex with a variety of binding partners,[12] insight into the role of dynamics in proteasome function and into the interaction of the CP with intrinsically disordered, and hence dynamic, substrates has not been forthcoming. One outstanding issue relates to the N-terminal tails of the α-subunits of the CP that are involved in substrate gating[11,13] and that are not visible in the X-ray structure[9] of the archaeal 20S CP. Studies using atomic force microscopy suggest that there is communication between the entrance gate and the active sites that are 75 Å removed,[14] yet structures of the yeast proteasome where the N-terminal 9 residues of one of the α subunits were removed showed little changes in regions distal from this site.[13] It is of significant interest to establish whether these two functional areas are dynamically coupled and in principle nuclear magnetic resonance (NMR) spectroscopy is especially well suited to address this question. In practice, however, applications of NMR methodology have been limited to relatively small proteins.

Our laboratory has initiated a study of the 20S CP from the Archaeon *Thermoplasma acidophilum* in an attempt to clarify the relation between dynamics and function in this system.[15] Central to our efforts has been the use of a labeling strategy where highly deuterated proteins are produced, with protonation confined to one of the two methyl groups of Leu and Val residues and to the Cδ position of Ile.[16] In concert, NMR

(1) Karplus, M.; Kuriyan, J. *Proc. Natl. Acad. Sci. U.S.A.* **2005**, *102*, 6679−6685.
(2) Wand, A. J. *Nat. Struct. Biol.* **2001**, *8*, 926−931.
(3) Eisenmesser, E. Z.; Millet, O.; Labeikovsky, W.; Korzhnev, D. M.; Wolf-Watz, M.; Bosco, D. A.; Skalicky, J. J.; Kay, L. E.; Kern, D. *Nature* **2005**, *438*, 117−121.
(4) Mulder, F. A. A.; Mittermaier, A.; Hon, B.; Dahlquist, F. W.; Kay, L. E. *Nat. Struct. Biol.* **2001**, *8*, 932−935.
(5) Kay, L. E.; Muhandiram, D. R.; Wolf, G.; Shoelson, S. E.; Forman-Kay, J. D. *Nat. Struct. Biol.* **1998**, *5*, 156−163.
(6) Kern, D.; Zuiderweg, E. R. *Curr. Opin. Struct. Biol.* **2003**, *13*, 748−757.
(7) Pickart, C. M.; Cohen, R. E. *Nat. Rev. Mol. Cell Biol.* **2004**, *5*, 177−187.
(8) Baumeister, W.; Walz, J.; Zuhl, F.; Seemuller, E. *Cell* **1998**, *92*, 367−380.
(9) Lowe, J.; Stock, D.; Jap, B.; Zwickl, P.; Baumeister, W.; Huber, R. *Science* **1995**, *268*, 533−539.
(10) Unno, M.; Mizushima, T.; Morimoto, Y.; Tomisugi, Y.; Tanaka, K.; Yasuoka, N.; Tsukihara, T. *Structure* **2002**, *10*, 609−618.
(11) Groll, M.; Ditzel, L.; Lowe, J.; Stock, D.; Bochtler, M.; Bartunik, H. D.; Huber, R. *Nature* **1997**, *386*, 463−471.
(12) Whitby, F. G.; Masters, E. I.; Kramer, L.; Knowlton, J. R.; Yao, Y.; Wang, C. C.; Hill, C. P. *Nature* **2000**, *408*, 115−120.
(13) Groll, M.; Bajorek, M.; Kohler, A.; Moroder, L.; Rubin, D. M.; Huber, R.; Glickman, M. H.; Finley, D. *Nat. Struct. Biol.* **2000**, *7*, 1062−1067.
(14) Osmulski, P. A.; Gaczynska, M. *Biochemistry* **2002**, *41*, 7047−7053.
(15) Sprangers, R.; Kay, L. E. *Nature*, in press.

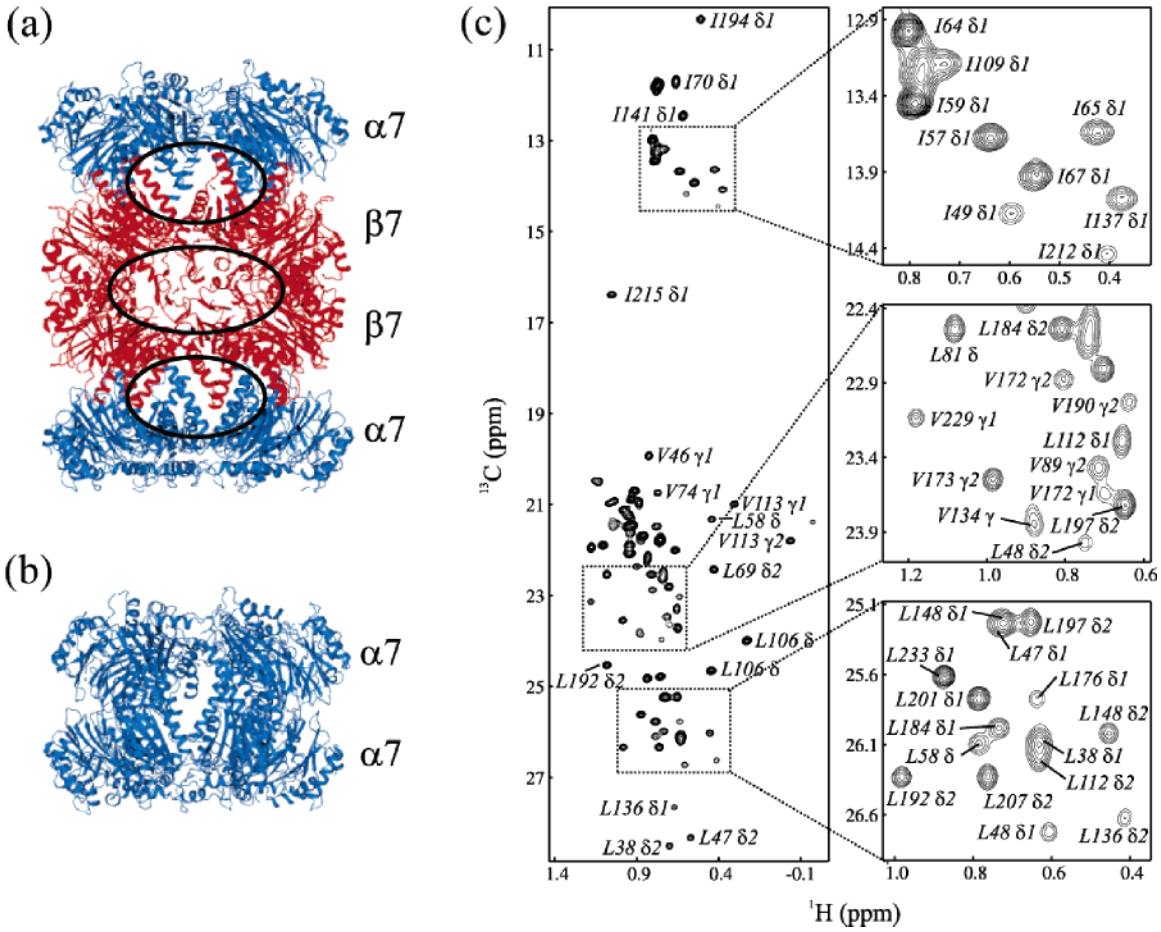

Figure 1. Ribbon diagrams of the 20S CP (a, $\alpha_7\beta_7\beta_7\alpha_7$) and the $\alpha_7\alpha_7$ "half-proteasome" (b) with the α and β subunits in blue and red, respectively. Each ring is comprised of 7 subunits.[9] The two antechambers and the catalytic chamber are indicated by ovals in (a). The $^1H-^{13}C$ HMQC correlation map of {U-[^2H]; Ileδ1-[$^{13}CH_3$]; Leu,Val-[$^{13}CH_3$,$^{12}CD_3$]}-labeled WT $\alpha_7\alpha_7$ is shown in **(c)**, recorded at 600 MHz, 50 °C. Site- specific assignments are available for 95% of the correlations[15] and many are indicated on the figure.

methodology has been developed that exploits the slow decay of 50% of the magnetization derived from methyl groups in slowly tumbling molecules (such as proteins) that gives rise to the so-called methyl-TROSY effect.[17] Site-specific assignments for 90% of the Ile (Cδ1), Leu, and Val methyls from α-rings of the 20S CP have been obtained and for 95% of the corresponding methyls in a 360 kDa particle that consists only of α-rings,[15] arranged in an $\alpha_7\alpha_7$ architecture (referred to as $\alpha_7\alpha_7$), Figure 1b,c. These assignments form the basis of all future studies. Preliminary studies of interactions of the 20S CP and $\alpha_7\alpha_7$ with targets have been undertaken and millisecond (ms) time-scale dynamics have been probed,[15] all making use of the {U-[^2H]; Ileδ1-[$^{13}CH_3$]; Leu,Val-[$^{13}CH_3$,$^{12}CD_3$]}-labeling strategy described above; it would clearly be advantageous if investigations of ps−ns protein dynamics could also be undertaken with the same samples and performed as a matter of course as part of the initial experiments that follow the assignment.

We have recently described a set of experiments that quantifies cross-correlated relaxation between intra-methyl $^1H-^1H$ dipolar interactions in highly deuterated, methyl protonated proteins that can be directly related to amplitudes of motion of methyl containing side-chains.[18] The approach was demonstrated with applications to proteins with molecular weights of up to 80 kDa, but for larger proteins, including the system that we are interested in here, sensitivity is limiting. With this in mind, we present a related set of experiments with significantly improved signal-to-noise. The approach is first validated with applications to protein L (7 kDa) and malate synthase G (MSG, 82 kDa), followed by a study of side-chain ps-ns time-scale dynamics in WT $\alpha_7\alpha_7$ and in a variant where the first 12 N-terminal residues, that comprise the proteasome gate, are deleted (Δ1−12 $\alpha_7\alpha_7$). The strong correlation (>0.99) between methyl-containing side-chain order parameters derived from the WT and truncated versions of $\alpha_7\alpha_7$ strongly suggests that truncation of the dynamic N-terminus has little effect on rapid side-chain dynamics in the rest of the α-ring.

Materials and Methods

NMR Samples. Relaxation studies were performed on {U-[^{15}N,^2H]; Ileδ1-[$^{13}CH_3$]; Leu,Val-[$^{13}CH_3$,$^{12}CD_3$]}-labeled samples of the B1 immunoglobulin binding domain of peptostreptoccocal protein L (7.5 kDa), malate synthase G (MSG, 82 kDa) and both WT and 12 residue N-terminal deletion versions of a "half-proteasome" $\alpha_7\alpha_7$ (360 kDa). All samples were prepared as described in detail previously[15,16,19,20] using U-[^2H]-D-glucose as the main carbon source and the appropriate α-keto-acid precursors for selective methyl labeling.[16,21] Sample conditions

(16) Tugarinov, V.; Kay, L. E. *J. Biomol. NMR* **2004**, *28*, 165−172.
(17) Tugarinov, V.; Hwang, P.; Ollerenshaw, J.; Kay, L. E. *J. Am. Chem. Soc.* **2003**, *125*, 10420−10428.
(18) Tugarinov, V.; Kay, L. E. *J. Am. Chem. Soc.* **2006**, *128*, 7299−7308.
(19) Mittermaier, A.; Kay, L. E. *J. Am. Chem. Soc.* **2001**, *123*, 6892−6903.
(20) Korzhnev, D. M.; Kloiber, K.; Kanelis, V.; Tugarinov, V.; Kay, L. E. *J. Am. Chem. Soc.* **2004**, *126*, 3964−3973.

were: 1.4 mM protein, 99.9% D_2O, 50 mM sodium phosphate, pH 6.0 (uncorrected) for protein L; 0.5 mM protein, 99.9% D_2O, 25 mM sodium phosphate, pH 7.1 (uncorrected), 20 mM $MgCl_2$, 0.05% NaN_3, 5 mM DTT for MSG; 0.14 mM protein (concentration of complex), 99.9% D_2O, 25 mM potassium phosphate, pH 6.8 (uncorrected), 50 mM NaCl, 1 mM EDTA, 0.03% NaN_3 and 2 mM DTT for both $\alpha_7\alpha_7$ samples.

NMR Spectroscopy and Data Analysis. Studies of Protein L were performed on a 500 MHz Varian Inova spectrometer equipped with a room-temperature probe-head, whereas all remaining experiments were conducted at 600 MHz using a spectrometer with a cryogenically cooled probe. Data sets for protein L, MSG, and the proteasome were recorded at 5, 37, and 50 °C, respectively, with parametrically varied delays T of 2, 7, 12, 17, 22, 27, 32, 37, 42 ms (protein L), 1, 2, 3, 4, 6, 8, 10, 14 ms (MSG), and 0.5, 0.7, 1, 1.5, 2, 3, 4, 5, 6, 7, 8, 10, 12, 14, 18, 22 ms (proteasome) and evolution times of 64(64) ms (protein L), 47(64) ms (MSG), and 45(64) ms (proteasome) in $t_1(t_2)$. Net acquisition times for each 2D data set recorded on (protein L, MSG, proteasome) samples were (1.1, 3.8, 3.8) hours and (1.1, 1.9, 1.9) hours for the 2Q and the biexponential relaxation experiments described below, respectively.

All NMR spectra were processed and analyzed using the NMRPipe/NMRDraw suite of programs[22] and associated home-written software. Intra-methyl $^1H-^1H$ dipolar cross-correlated relaxation rates η have been obtained by fitting the ratios of peak intensities measured in a pair of data sets recorded for each T value, (I_a/I_b) see below, to a modified *tanh* build-up function described in Results and Discussion. Errors in the extracted values of η were estimated by a Monte Carlo analysis[23] using random noise in spectra to obtain experimental uncertainties in I_a/I_b ratios.

Extraction of absolute order parameters from relaxation data requires an estimate of the overall molecular tumbling time. Values of diffusion tensors for protein L (at 5 °C) and MSG (at 37 °C) in D_2O were estimated as described in detail previously.[18,24] In the analysis of relaxation data for protein L, we have used a correlation time, τ_C, of 10.2 ns (assumed isotropic),[25,26] whereas $\tau_{C,eff} = (2D_{||} + 4D_{\perp})^{-1} =$ 41.4 ns has been used for MSG, along with $D_{||}/D_{\perp} = 1.21$ and polar angles $\theta = 13°$, $\phi = 48°$ describing the orientation of the unique diffusion axis relative to the inertia frame.[18] We have not measured the correlation time directly for the proteasome because ^{15}N-based correlation experiments are of low quality for this system, although calculations using hydrodynamic programs do establish that $\alpha_7\alpha_7$ tumbles as a sphere in solution.[15] Instead, a correlation time was "chosen" ($\tau_C = 120$ ns, 50 °C) so that all values of S^2_{axis} extracted from ^{13}C spin relaxation measurements on a $^{13}CHD_2$-labeled sample described elsewhere[15] are within [0−1]. Subsequently, correlation times for other half-proteasome samples have been corrected for changes in viscosity (due to differences in protein concentration) by the relation τ_C(sample) $= 120D_{CHD2}/D_{CH3}$, where D_{CHD2} is the protein translational diffusion constant measured in the sample used for ^{13}C relaxation studies ($\tau_C =$ 120 ns) and D_{CH3} is the diffusion constant measured on the sample of interest in the present application. Values of τ_C of 109 ns were obtained in this way for samples of both WT $\alpha_7\alpha_7$ and $\Delta1-12$ $\alpha_7\alpha_7$ used in the present set of ^1H relaxation experiments.

Results and Discussion

NMR Methodology. Figure 2 shows an energy level diagram and the corresponding ^1H transitions of interest for an isolated methyl group. In the limit that the methyl group is attached to a macromolecule and assuming very rapid rotation about the methyl 3-fold axis and that the motions that contribute to transverse relaxation are those that reflect the overall tumbling, it has been shown that the relaxation of each of the single quantum ^1H coherences, denoted by the vertical solid lines in the diagram, occurs in a single- exponential manner[17,27,28] with fast ($R^F_{2,H}$, blue) or slow ($R^S_{2,H}$, red) rates, depending on the transition. It has also been shown that the intra-methyl $^1H-^1H$ dipolar cross-correlated relaxation rate η is given by[18]

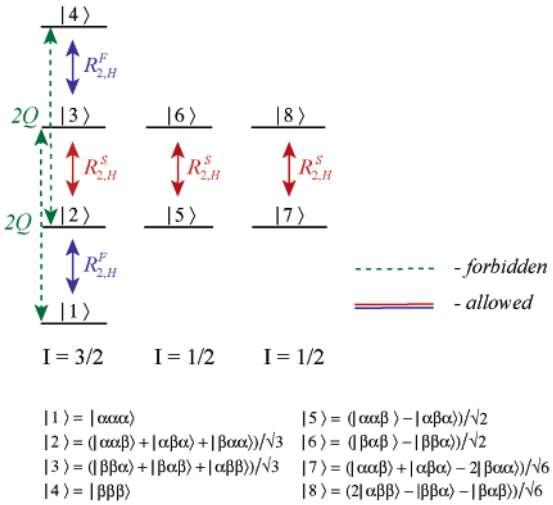

Figure 2. Energy level diagram for the X_3 spin-system of a methyl group. Slow(fast) relaxing single quantum ("allowed") ^1H transitions are labeled $R^S_{2,H}(R^F_{2,H})$ and are shown with red(blue) solid arrows. Double-quantum ("forbidden", 2Q) transitions are shown with dashed green arrows. The eight ^1H eigenstates are depicted by $|i,j,k\rangle$ ($i,j,k \in \{\alpha,\beta\}$).

$$\eta = \frac{R^F_{2,H} - R^S_{2,H}}{2} \approx \frac{9}{10}[P_2(\cos\theta_{axis,HH})]^2 \frac{S^2_{axis}\gamma^4_H\hbar^2\tau_C}{r^6_{HH}} \quad (1)$$

where τ_c is the tumbling time, γ_H is the gyromagnetic ratio of a proton spin, r_{HH} is the distance between pairs of methyl protons[18,29] (1.813 Å), S_{axis} is the generalized order parameter describing the amplitude of motion of the methyl 3-fold axis, $P_2(x) = (1/2)(3x^2 - 1)$, and $\theta_{axis,HH}$ (90°) is the angle between the methyl 3-fold axis and a vector that connects a pair of methyl ^1H nuclei. For a detailed general account of cross-correlated spin relaxation with some discussion of methyl groups, the reader is referred to papers by Werbelow and Grant[30] and Vold and Vold.[31]

Our goal in what follows is to measure η and hence S_{axis} by exploiting what has been referred to by Ernst, Wokaun, and Bodenhausen as the "forbidden fruits of NMR spectroscopy".[32] Here we make use of relaxation violated coherence transfer,[27,28] whereby methyl proton double quantum (2Q) coherences can be prepared on the basis of $\eta \neq 0$ despite the fact that (^{13}C

(21) Tugarinov, V.; Kay, L. E. *Chembiochem* **2005**, *6*, 1567−1577.
(22) Delaglio, F.; Grzesiek, S.; Vuister, G. W.; Zhu, G.; Pfeifer, J.; Bax, A. *J. Biomol. NMR* **1995**, *6*, 277−293.
(23) Kamith, U.; Shriver, J. W. *J. Biol. Chem.* **1989**, *264*, 5586−5592.
(24) Tugarinov, V.; Ollerenshaw, J. E.; Kay, L. E. *J. Am. Chem. Soc.* **2005**, *127*, 8214−8225.
(25) Skrynnikov, N. R.; Millet, O.; Kay, L. E. *J. Am. Chem. Soc.* **2002**, *124*, 6449−6460.
(26) Tugarinov, V.; Kay, L. E. *J. Biomol. NMR* **2004**, *29*, 369−376.
(27) Müller, N.; Bodenhausen, G.; Ernst, R. R. *J. Magn. Reson.* **1987**, *75*, 297−334.
(28) Kay, L. E.; Prestegard, J. H. *J. Am. Chem. Soc.* **1987**, *109*, 3829−3835.
(29) Ishima, R.; Petkova, A. P.; Louis, J. M.; Torchia, D. A. *J. Am. Chem. Soc.* **2001**, *123*, 6164−6171.
(30) Werbelow, L. G.; Grant, D. M. *Adv. Magn. Reson.* **1977**, *9*, 189−299.
(31) Vold, R. R.; Vold, R. L. *J. Chem. Phys.* **1976**, *64*, 320−332.
(32) Ernst, R. R.; Bodenhausen, G.; Wokaun, A. *Principles of Nuclear Magnetic Resonance in One and Two Dimensions*; Oxford University Press: Oxford, 1987.

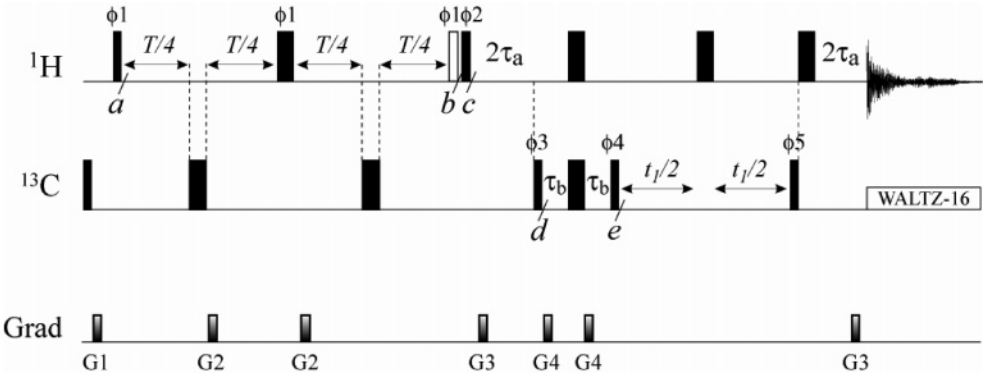

Figure 3. Pulse sequences for the measurement of intra-methyl $^1H-^1H$ dipolar cross-correlated relaxation rates, $\eta = (R^F_{2,H} - R^S_{2,H})/2$, in $^{13}CH_3$ methyl groups of highly deuterated proteins. The complete sequence is used to measure the build-up of 2Q coherences during T (resulting in correlations with intensities I_a) while a second experiment is recorded to measure the (biexponential) decay of ^1H single quantum magnetization during T by removing the (open) pulse at point b (correlations with intensities I_b). All narrow(wide) rectangular pulses are applied with flip angles of 90(180)° along the x-axis unless indicated otherwise. The ^1H and ^{13}C carrier frequencies are positioned in the center of the Ileδ1-Leu-Val methyl region—at 0.5 and 18 ppm, respectively. All ^1H and ^{13}C pulses are applied with the highest possible power, whereas ^{13}C WALTZ-16 decoupling[33] is achieved using a 2-kHz field. Delays are: $\tau_a = 1.8$ ms; $\tau_b = 1$ ms; T is a variable relaxation delay. The durations and strengths of pulsed-field z-gradients in units of (ms;G/cm) are: G1 = (1;5), G2 = (0.05;-20), G3 = (0.5;10), G4 = (0.15;12). The phase cycle is: $\phi1 = x,y,-x,-y$; $\phi2 = 4(x),4(-x)$; $\phi3 = 8(x),8(-x)$; $\phi4 = 4(y),4(-y)$; $\phi5 = x$; rec. = $2(x,-x)$, $4(-x,x)$, $2(x,-x)$ (2Q experiment), and $\phi1 = x,-x$; $\phi2 = 2(y),2(-y)$; $\phi3 = 8(x),8(-x)$; $\phi4 = 4(y),4(-y)$; $\phi5 = x$; rec. = $4(x,-x),4(-x,x)$ (decay of ^1H single quantum magnetization). Quadrature detection in F_1 is achieved via STATES-TPPI incrementation[34] of $\phi5$.

decoupled) ^1H NMR spectra of isolated methyl groups consist of a single line with no observed homonuclear scalar couplings. In the absence of relaxation or in the limit where $\eta = 0$, these 2Q coherences are disallowed, but they can be created efficiently in the case of methyl groups attached to macromolecules, as has been described previously.[28] We show below that the time dependence of the preparation of such 2Q coherences is a sensitive probe of dynamics, even in systems with molecular weights of hundreds of kDa, and that robust measures of motion can be obtained. Figure 3 illustrates the pulse schemes that have been developed for measuring the time-dependence of the buildup of 2Q coherences and the biexponential relaxation of transverse ^1H magnetization that are used in concert, as described below, to probe methyl group dynamics.

The experiment begins with a preparation period between points *a*-*b* during which the relaxation properties of the methyl group are explored and subsequently encoded in the intensities of correlations in $^1H-^{13}C$ spectra using an HMQC element that specifically selects for slowly relaxing multiplet components.[20] In what follows below, we first consider the case of an isolated methyl group, using a density matrix description that follows the notation previously introduced by Ollerenshaw et al.,[35] along with wavefunctions $|1> - |8>$ that are defined in Figure 2 (note that $|8>$ is defined differently from ref 35). In $|1> - |8>$ the ^1H spin states are depicted by $|i,j,k>$ ($i,j,k \in \{\alpha,\beta\}$), and we have neglected to include the ^{13}C spin because the important features of the experiment can be described simply by focusing on protons.

Consider first the experiment that creates 2Q coherences during T, given by the sequence of Figure 3 that includes the "open" pulse at point b, focusing on the case where $\phi1 = y$. After the first 90° pulse, the density matrix is given by

$$\rho_a = \sqrt{3}/2(|1><2| + |2><1| + |3><4| + |4><3|) + 1(|2><3| + |3><2|) + 1/2(|5><6| + |6><5| + |7><8| + |8><7|) \quad (2)$$

with the created transverse ^1H magnetization (pictured in Figure 2 with vertical arrows) subsequently evolving for a period T. During this interval evolution of ^1H magnetization due to chemical shift and $^1H-^{13}C$ scalar coupling is refocused, as are a number of cross-correlated spin-relaxation interactions such as those from $^1H-^{13}C/^1H-^1H$ dipolar interactions and $^1H-^1H$ dipolar/^1H chemical shift anisotropy. To an excellent approximation, the relaxation evolution of the spin system is dominated by $^1H-^1H$ dipolar (both auto- and cross-correlated) and $^1H-^{13}C$ dipolar (auto- and cross-correlated) interactions and for an isolated methyl group we can write,

$$\frac{d\vec{v}(t)}{dt} = -\tilde{D}\vec{v}(t)$$
$$\vec{v}^T(t) = (\rho_{12}, \rho_{23}, \rho_{34}, \rho_{56}, \rho_{78}) \quad (3)$$

where $\tilde{D} = diag(R^F_{2,H}, R^S_{2,H}, R^F_{2,H}, R^S_{2,H}, R^S_{2,H})$ is a diagonal 5×5 matrix, ρ_{ij} is the density element coupling states $|i>$ and $|j>$ of Figure 2, and $\vec{v}^T(t)$ is the transpose of vector $\vec{v}$ that contains the values of the five relevant density elements evaluated at time t. Equation 3 can be solved using the boundary conditions in eq 2, $\vec{v}^T(0) = (\sqrt{3}/2,1,\sqrt{3}/2,1/2,1/2)$, to give the values of the density elements at time T, $\vec{v}(T)$. Immediately after the 90° pulse at point b, the density terms of interest, corresponding to 2Q coherences (that are selected by phase cycling in the experiment), are given by

$$\rho_b = \rho_{12}(T)[-1/2(|1><3| + |3><1|) + 1/2(|2><4| + |4><2|)] + \rho_{23}(T)[\sqrt{3}/4(|1><3| + |3><1|) - \sqrt{3}/4(|2><4| + |4><2|)] \quad (4)$$

where $\rho_{ij}(T)$ is the $i-j$ density element at time T (i.e., the value of ρ_{ij} immediately before the ^1H pulse of phase $\phi1$ at point b). Note that only elements from the 3/2 manifold (Figure 2) contribute to 2Q coherences. The subsequent 90° pulse at point

(33) Shaka, A. J.; Keeler, J.; Frenkiel, T.; Freeman, R. *J. Magn. Reson.* **1983**, *52*, 335−338.
(34) Marion, D.; Ikura, M.; Tschudin, R.; Bax, A. *J. Magn. Reson.* **1989**, *85*, 393−399.
(35) Ollerenshaw, J. E.; Tugarinov, V.; Kay, L. E. *Magn. Reson. Chem.* **2003**, *41*, 843−852.

c converts the 2Q coherences to ^{1}H transverse magnetization where only the slowly relaxing transitions,

$$\rho_c = (\sqrt{3}/4\rho_{12}(T) - 3/8\rho_{23}(T))(|2><3| + |3><2|) \quad (5)$$

contribute to the observed signal because these only survive the filter between points d and e in Figure 3, as described previously.[20] Correlations at (ω_C, ω_H) are obtained using an HMQC scheme with intensities proportional to I_a,

$$I_a = \sqrt{3}/2\rho_{12}(T) - 3/4\rho_{23}(T) = 3/4\exp(-R^F_{2,H}T) - 3/4\exp(-R^S_{2,H}T) \quad (6)$$

A second experiment is also recorded that measures the decay of ^{1}H transverse magnetization where the 90° pulse at point b is omitted. Following the same analysis as above, immediately after the 90° pulse of phase $\phi 2$, the density elements of interest are those associated with slowly relaxing transverse ^{1}H magnetization,

$$\rho_c = (\sqrt{3}/2\rho_{12}(T) + 1/4\rho_{23}(T))(|2><3| + |3><2|) + \rho_{56}(T)(|5><6| + |6><5|) + \rho_{78}(T)(|7><8| + |8><7|). \quad (7)$$

Following the course of the magnetization until the end of the sequence we obtain correlations at (ω_C, ω_H) with intensities proportional to I_b,

$$I_b = \sqrt{3}\rho_{12}(T) + 1/2\rho_{23}(T) + \rho_{56}(T) + \rho_{78}(T) = 3/2\exp(-R^F_{2,H}T) + 3/2\exp(-R^S_{2,H}T) \quad (8)$$

Finally, we prefer to fit ratios of peak intensities obtained in the pair of experiments described above, I_a/I_b, to an equation of the form,

$$I_a/I_b = -1/2 \tanh(\eta T) \quad (9)$$

The above analysis pertains to an isolated methyl group. In practice, methyl groups in proteins are not isolated, even in cases where molecules are highly deuterated. In the case of {U-[^{2}H]; Ileδ1-[^{13}CH$_3$]; Leu,Val-[^{13}CH$_3$,^{12}CD$_3$]}-labeled MSG, for example, an average effective intra-methyl distance of 2.9 Å is calculated, with a minimum distance of 1.9 Å (i.e., if all protons in the protein, excluding the methyl in question, could be replaced by a single proton, its distance would be 2.9 Å, on average, to the methyl). We have chosen the simplest approach for modeling relaxation involving external spins, where we assume that contributions to relaxation of a given methyl group can be obtained simply by summing up individual contributions from each external proton. Cross-correlation effects between different external spin interactions involving a single methyl site are not included although for each external proton-methyl group interaction the effects of cross-correlation are included. External protons can be taken into account by modifying eq 3 according to

$$\frac{d\vec{v}'(t)}{dt} = -(\tilde{D}' + \tilde{E})\vec{v}'(t) \quad (10)$$

where $\tilde{D}' = \mathrm{diag}(R^F_{2,H}, R^S_{2,H}, R^F_{2,H}, R^S_{2,H})$ and the matrix $\tilde{E}$ accounts for the external protons. We showed in a previous publication that[18]

$$\tilde{E} = k_{HH}\begin{bmatrix} 9 & 0 & 0 & 0 \\ 0 & 9 & -4 & 2\sqrt{2} \\ 0 & -4 & 9 & -2\sqrt{2} \\ 0 & 2\sqrt{2} & -2\sqrt{2} & 7 \end{bmatrix}$$

$$k_{HH} = \sum_{ext}\left(\frac{1}{20}\right)\frac{\hbar^2\gamma_H^4\tau_C}{r^6_{HHext}} \quad (11)$$

and

$$\vec{v}'^{,T} = \left(\frac{\rho_{34} - \rho_{12}}{\sqrt{2}}, \frac{2\rho_{23} + \rho_{56} + \rho_{78}}{\sqrt{6}}, \frac{\rho_{34} + \rho_{12}}{\sqrt{2}}, \frac{\rho_{23} - \rho_{56} - \rho_{78}}{\sqrt{3}}\right)$$

Equations 10−11 imply that $\rho_{12}(T) = \rho_{34}(T)$ and an approximate analytical solution can be obtained in a straightforward manner by noting from eq 2 that $\vec{v}'^{,T}(0) = (0,\sqrt{6}/2,\sqrt{6}/2,0)$ and assuming that $\rho_{23}(T) \approx \rho_{56}(T) + \rho_{78}(T)$ for all T. The time dependence of the terms of interest can thus be calculated from

$$\frac{d\vec{y}(t)}{dt} = -\tilde{M}\vec{y}(t) \quad (12)$$

where

$$\vec{y}^T = \left(\frac{2\rho_{23} + \rho_{56} + \rho_{78}}{\sqrt{6}}, \frac{\rho_{34} + \rho_{12}}{\sqrt{2}}\right)$$

$$M = \begin{pmatrix} R^S_{2,H} + R_{ext} & \delta \\ \delta & R^F_{2,H} + R_{ext} \end{pmatrix},$$

$R_{ext} = 9k_{HH}$ and $\delta = -4k_{HH}$. Following a straightforward derivation as above, we obtain the following expression for I_a/I_b,

$$I_a/I_b = \frac{-0.5\eta \tanh(\sqrt{\eta^2 + \delta^2}T)}{\sqrt{\eta^2 + \delta^2} - \delta \tanh(\sqrt{\eta^2 + \delta^2}T)} \quad (13)$$

It is worth noting that in the derivation of eq 13, we have considered relaxation effects rigorously only during the period T in the sequence of Figure 3. An analysis that includes relaxation during the HMQC portion as well establishes that this is an excellent approximation so long as $\rho_{23}(T) \approx \rho_{56}(T) + \rho_{78}(T)$, as was assumed in the derivation. We show subsequently that values of S_{axis} obtained from fits to eq 13 are in very good agreement with those extracted from either ^{13}C or ^{2}H relaxation data sets.

Experimental Verification. Equation 13 shows that the ratio of the intensities of correlations measured in the experiments of Figure 3 (i.e., with and without the open pulse) is related to the intra-methyl ^{1}H−^{1}H dipole cross-correlated relaxation rate, η, and to a cross-relaxation parameter, δ, that depends on the proximity of external protons to the methyl group in question. Typically, values of η, and hence of S^2_{axis} (see eq 1), are obtained by fitting the time dependence of I_a/I_b to eq 13, as shown in Figure 4 for a number of residues in protein L (a)

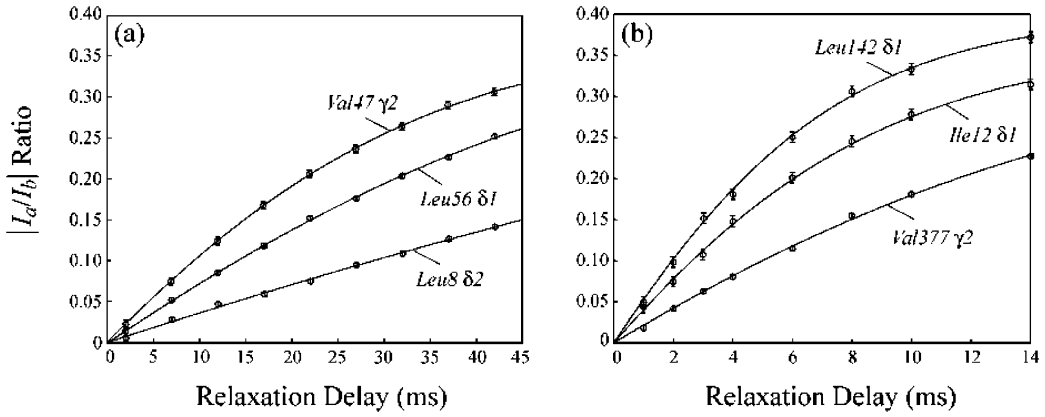

Figure 4. Build-up curves of experimental $|I_a/I_b|$ intensity ratios best-fit to the theoretical $|I_a/I_b|$ ratio as given by eq 13 for (a) Leu8 $\delta 2$, Val47 $\gamma 2$ and Leu56 $\delta 1$ methyl groups of {U-[^{15}N,^{2}H]; Ileδ1-[$^{13}CH_3$]; Leu,Val-[$^{13}CH_3$,$^{12}CD_3$]}-protein L (500 MHz, 5 °C); (b) Ile12 $\delta 1$, Leu142 $\delta 1$ and Val377 $\gamma 2$ methyls of {U-[^{15}N,^{2}H]; Ileδ1-[$^{13}CH_3$]; Leu,Val-[$^{13}CH_3$,$^{12}CD_3$]}-MSG (600 MHz, 37 °C).

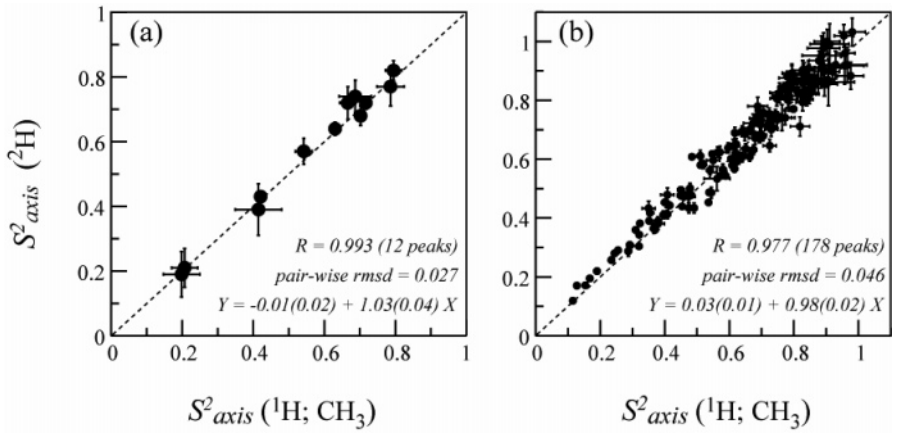

Figure 5. (a) Linear correlation plot of ^{2}H-derived S^2_{axis} values (y-axis) of Ile(δ1), Leu, Val methyl groups in protein L (ref 25) vs S^2_{axis} values obtained from cross-correlation rates η in {U-[^{15}N,^{2}H]; Ileδ1-[$^{13}CH_3$]; Leu,Val-[$^{13}CH_3$,$^{12}CD_3$]}-labeled protein L (x-axis). (b) As in (a) but with η values measured on {U-[^{15}N,^{2}H]; Ileδ1-[$^{13}CH_3$]; Leu,Val-[$^{13}CH_3$,$^{12}CD_3$]}-labeled MSG and S^2_{axis}(^{2}H) values derived from $R(^{13}CHD_2)$ measurements.[37] See text for the parameters of methyl geometry used to obtain ^{1}H relaxation-derived values of S^2_{axis}. Best-fit parameters from a linear regression analysis of the data are shown for each plot along with Pearson correlation coefficients, R, obtained for the number of data points (peaks) indicated in parentheses and the pairwise rmsd of S^2_{axis} values measured via the different approaches. Dashed lines corresponding to $y = x$ are indicated.

and MSG (b). Average values ($\pm$1 standard deviation) of η are 22 ± 7 s^{-1} and 98 ± 31 s^{-1} for protein L (5 °C) and MSG (37 °C).

Figure 5 plots S^2_{axis}values measured from ^{2}H-based spin relaxation experiments recorded on samples where Ile, Leu and Val methyls are of the $^{13}CH_2D$ (a, Protein L)[25,36] or $^{13}CHD_2$ (b, MSG)[37] variety vs S^2_{axis} values obtained using the methodology described here where {U-[^{2}H]; Ileδ1-[$^{13}CH_3$]; Leu,Val-[$^{13}CH_3$,$^{12}CD_3$]}-labeled protein L or MSG samples have been studied. Very good correlations are noted between the different data sets, establishing that robust measures of methyl side chain order can be obtained using ^{1}H spin relaxation, even when a simple model is used to account for the influence of external contributions to relaxation.

Extracted values of δ are also obtained from the fits. All values are negative, as expected (eq 12), and there is an acceptable correlation with values calculated using the X-ray coordinates of both proteins; Pearson's R of 0.8, 0.85 and 0.5 for correlations involving data from protein L, MSG (a sample where only Ile δ1 methyls were protonated) and MSG (Ileδ1,

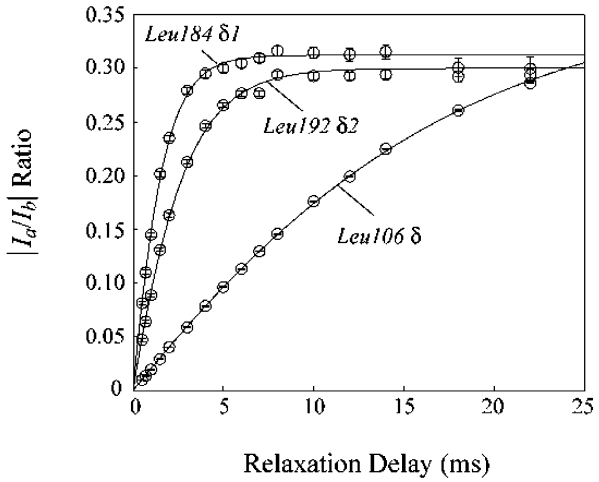

Figure 6. Build-up curves of $|I_a/I_b|$ intensity ratios fit to the theoretical ratio, eq 13 for Leu106 δ, Leu184 $\delta 1$ and Leu192 $\delta 2$ of {U-[^{15}N,^{2}H]; Ileδ1-[$^{13}CH_3$]; Leu,Val-[$^{13}CH_3$,$^{12}CD_3$]}-WT $\alpha_7\alpha_7$ (600 MHz, 50 °C).

Leu and Val protonated methyls), respectively. However, the effective distance to external proton spins, $r_{eff} = (\sum_{ext} 1/r^6_{HHext})^{-1/6}$, that is calculated from the extracted δ values is, on average, somewhat smaller than the average value

(36) Millet, O.; Muhandiram, D. R.; Skrynnikov, N. R.; Kay, L. E. *J. Am. Chem. Soc.* **2002**, *124*, 6439−6448.
(37) Tugarinov, V.; Kay, L. E. *Biochemistry* **2005**, *44*, 15970−15977.

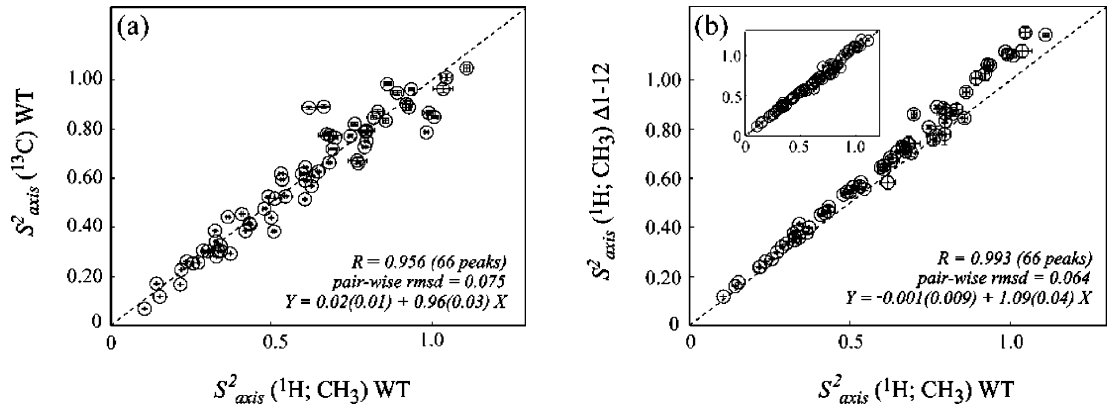

Figure 7. (a) Correlation of S^2_{axis} values obtained from (i) ^{13}C relaxation measurements recorded on a $^{13}CHD_2$-labeled WT-$\alpha_7\alpha_7$ sample[15] (*y*-axis) and from (ii) a ^{1}H relaxation study of a {U-[^{15}N,^{2}H]; Ileδ1-[$^{13}CH_3$]; Leu,Val-[$^{13}CH_3$,$^{12}CD_3$]}-WT $\alpha_7\alpha_7$ complex (600 MHz, 50 °C). (b) Correlation of Ile, Leu and Val methyl S^2_{axis} values of WT and Δ1−12 $\alpha_7\alpha_7$ complexes obtained from ^{1}H relaxation measurements (600 MHz, 50 °C). All ^{1}H experiments in (a) and (b) used the schemes of Figure 3. Dashed lines corresponding to $y = x$ are shown. The inset to (b) shows the same correlation as in (b) but with the best fit line $y = 1.09x$, emphasizing that the relative degrees of order at the methyl positions in the two molecules are essentially identical.

predicted (2.7 vs 3.4 Å). The elevated δ values likely result from the overly simplistic model that has been used to derive eq 13 where it has been assumed that all slowly relaxing ^{1}H transitions are affected equally from external proton spins ($\rho_{23}(T) = \rho_{56}(T) + \rho_{78}(T)$, above). Certainly more sophisticated models can be used, but then relaxation throughout the course of the entire pulse scheme must be accounted for, introducing a degree of complexity that we feel is not warranted given the good correlation of S^2_{axis} values in Figure 5.

Application to $\alpha_7\alpha_7$. As described above and illustrated in Figure 1a, the proteasome has a barrel structure comprised of four rings,[9] two α and two β. In the case of the archaeal version studied here, each of the rings is made up of 7 identical repeats of equivalent α or β subunits. Wild-type α subunits produced in the absence of the β particle assemble to form an $\alpha_7\alpha_7$ "half-proteasome," and this is a particularly useful property for biophysical studies because $\alpha_7\alpha_7$ is only approximately half the molecular weight of the full 20S CP and, hence, gives better spectra and because it can be produced in significantly higher quantities than the 20S CP. Our previous studies have shown that ms and ps−ns side-chain dynamics of methyl-containing residues in the α-particle are similar for both $\alpha_7\alpha_7$ and $\alpha_7\beta_7\beta_7\alpha_7$, with a few exceptions for residues that are localized to the α/β interface.[15] Thus, $\alpha_7\alpha_7$ is a good model system for the study of dynamics of α particles in the context of the 20S CP.

With this in mind we have measured S^2_{axis} values using the methods described above on a pair of {U-[^{2}H]; Ileδ1-[$^{13}CH_3$]; Leu,Val-[$^{13}CH_3$,$^{12}CD_3$]}-samples, including WT $\alpha_7\alpha_7$ and a second sample where the first 12 N-terminal residues of the α-subunit have been truncated (Δ1−12 $\alpha_7\alpha_7$). These residues make up a "gate" that prevents entry of folded and many unfolded proteins into the chamber of the proteasome and there is interest in establishing whether the gate "communicates" with other regions of the structure, perhaps through a network of residues with coupled dynamics. Insight can be provided through a comparison of extracted methyl containing side-chain order parameters in the two forms of the molecule mentioned above.

Figure 6 shows the time dependence of $|I_a/I_b|$ measured for residues Leu106 δ (stereo-assignment not available), Leu184 δ1 and Leu192 δ2 in WT $\alpha_7\alpha_7$, along with the fit to the theoretical buildup for $|I_a/I_b|$, eq 13 (solid line). Not surprisingly, for the majority of residues in WT $\alpha_7\alpha_7$ plateau values in the build-up are reached at shorter delays than for protein L or MSG (compare Figures 4 and 6). Nevertheless, there are a number of highly dynamic residues in the half-proteasome (such as Leu106) and in order to quantify their motional properties properly we have chosen to extend the relaxation delays to values somewhat larger than those used for MSG. Average η values of 234 ± 101 (50 °C) are obtained. It is clear that high quality data can be obtained despite the fact that the molecular weight of the complex is 360 kDa.

We have recently measured S^2_{axis} values in WT $\alpha_7\alpha_7$ using both ^{13}C and ^{2}H spin relaxation in $^{13}CHD_2$ methyl groups and have shown that there is an excellent correlation between the two sets of measurements[15] (Pearson correlation coefficient of 0.95, pairwise rmsd of 0.05). Figure 7a compares S^2_{axis} values from the ^{13}C relaxation data set with values obtained by quantifying ^{1}H−^{1}H cross-correlation and the good agreement between data sets validates the ^{1}H-based measurements on this system. A comparison of order parameters for WT $\alpha_7\alpha_7$ and Δ1−12 $\alpha_7\alpha_7$, measured using the approach described here, is presented in Figure 7b; although values of S^2_{axis} are approximately 10% higher for Δ1−12 $\alpha_7\alpha_7$, the pairwise rmsd of S^2_{axis} values between data sets (0.06) is still less than between ^{1}H- and ^{13}C-derived S^2_{axis} for WT $\alpha_7\alpha_7$ (0.07), Figure 7a. The 10% elevation likely reflects the fact that order parameters are extracted from measurements on separate samples with slight variations in conditions that can be difficult to completely take into account. Nevertheless, it is very clear that the relative methyl dynamics in $\alpha_7\alpha_7$ do not change upon truncation of the gate residues as shown in the inset to Figure 7b where the best fit line through the data is plotted. Thus, it appears unlikely that the proteasome gate plays a role in any dynamic network that might be involved in communicating with distal regions of the protein, at least not on the ps-ns time-scale. Comparative studies of ms time-scale motions in both WT $\alpha_7\alpha_7$ and Δ1−12 $\alpha_7\alpha_7$ also indicate very little change in slower dynamics as well.[15]

Comparison with Other Methods. As described in the introduction, the primary advantage of the present methodology is that it can be applied to samples that are likely available at a very early stage from other studies. In our laboratory, studies of supra-molecular complexes routinely involve the production

of {U-[^{2}H]; Ileδ1-[$^{13}CH_3$]; Leu,Val-[$^{13}CH_3$,$^{12}CD_3$]}-labeled samples, which can then be used to measure side-chain methyl dynamics, as demonstrated here. Although we have previously published methods for obtaining S^2_{axis} values that are based on ^{1}H relaxation measurements that quantify $R^F_{2,H}$ and $R^S_{2,H}$ rates separately using [$^{13}CH_3$,$^{12}CD_3$]-labeled molecules, the present approach offers significant sensitivity advantages. Notably, both ^{1}H-based methods involve measurement of a pair of data sets, with one significantly less sensitive than the other; in the present scheme the least sensitive data set measures the build-up of DQ coherences, while among the experiments that measure $R^F_{2,H}$ and $R^S_{2,H}$ separately, the former is the least sensitive.[18] One way of assessing sensitivity would be to compare the average signal-to-noise values obtained in these two "sensitivity limiting" experiments. In applications involving MSG the average signal-to-noise obtained in the data set recorded with a T value that gives the maximum build-up of DQ coherences is approximately 2-fold greater than that of the maximum sensitivity data set ($T = 0$) used to measure $R^F_{2,H}$ directly. This leads to the higher proportion of methyl groups whose dynamics could be quantified for MSG in this study, 178 vs 131. In applications to $\alpha_7\alpha_7$ where τ_C is approximately a factor of 3 larger than for MSG the difference in the relative sensitivity of the limiting data sets will be significantly larger than for MSG, so that the present method is the only one feasible for studies of side-chain dynamics via ^{1}H spin relaxation.

There are a number of disadvantages associated with ^{1}H-based experiments, however. First, we were not able to reproduce S^2_{axis} values obtained from ^{2}H spin relaxation measurements (that have been extensively cross-validated) for proteins with correlation times less than approximately 10 ns. This has been noted previously in our studies of side-chain dynamics via measurement of intra-methyl ^{1}H-^{1}H cross-correlation[18] or intra-methyl ^{1}H$-^1$H/^{1}H$-^{13}$C cross-correlated relaxation.[26] Second, methods that are based on ^{1}H relaxation are often sensitive to external ^{1}H spins that can complicate extraction of meaningful dynamics parameters. Although excellent agreement between S^2_{axis} values measured using the present methodology and values obtained via ^{2}H and ^{13}C spin relaxation is demonstrated here, the fact that extracted values of δ are larger than expected is an important reminder of the difficulties in using ^{1}H relaxation as a probe, in general. In this regard, it is important to restate that our studies have been done with highly deuterated proteins that minimize but do not eliminate contributions from external protons. Finally, in comparing ^{2}H-, ^{13}C-, and ^{1}H-derived measures of order the ^{2}H and ^{13}C measurements have some advantages, notwithstanding the fact that additional samples must be prepared. In the limit of high signal-to-noise, the ^{2}H approach is preferred since the robustness of the data can often be established through a suite of experiments that cross-validates the measured rates[36] (at least for $^{13}CH_2D$ probes) and since the relaxation is dominated by the quadrupolar effect.[38] In contrast, for applications to supra-molecular systems ^{13}C measurements are of much higher sensitivity than either ^{1}H or ^{2}H; we estimate that on average the sensitivity per unit measuring time of the methodology presented here is similar to that of the ^{2}H experiments ($^{13}CHD_2$ label) with a 3- and 5-fold decrease relative to ^{13}C approaches for MSG ($\tau_C \approx 40$ ns) and $\alpha_7\alpha_7$ ($\tau_C \approx 120$ ns), respectively. Indeed, in some applications it is likely that only ^{13}C based experiments will be of sufficient sensitivity to extract precise values of S^2_{axis}.

In summary, we have presented pulse schemes for the measurement of order parameters characterizing ps-ns time-scale motions of Ile, Leu, and Val methyl groups in highly deuterated large proteins. The experiments make use of {U-[^{2}H]; Ileδ1-[$^{13}CH_3$]; Leu,Val-[$^{13}CH_3$,$^{12}CD_3$]}-labeled samples that, at least in our laboratory, form the basis for many studies of high molecular weight proteins. The approach has been validated by comparing S^2_{axis} values obtained using a number of different techniques that exploit different spin probes and a number of proteins. A comparative study of ps$-$ns dynamics of Ile, Leu, and Val side-chains of WT $\alpha_7\alpha_7$ and Δ1$-$12 $\alpha_7\alpha_7$ suggests that the gating residues in the proteasome do not communicate with other regions of the molecule via motions on this time-scale. This work provides another illustration of the fact that detailed, quantitative information of the sort normally reserved for NMR applications to small proteins can be obtained in studies of supra-molecular structures so long as labeling schemes and experiments are optimized appropriately.

Acknowledgment. This work was supported by Canadian Institutes of Health Research (CIHR) and Natural Sciences and Engineering Research (NSERC) grants to L.E.K. and by postdoctoral fellowships from the CIHR (V.T.) and the CIHR Strategic Training Program in Protein Folding: Principles and Diseases (R.S.). L.E.K. holds a Canada Research Chair in Biochemistry.

Supporting Information Available: S^2_{axis} values for protein L, MSG, and $\alpha_7\alpha_7$ that are used to generate Figures 5a, 5b, and Figure 7a of the text, presented in tabular form. This material is available free of charge via the Internet at http://pubs.acs.org.

JA067827Z

(38) Muhandiram, D. R.; Yamazaki, T.; Sykes, B. D.; Kay, L. E. *J. Am. Chem. Soc.* **1995**, *117*, 11536−11544.